

The following article has been submitted to *APL Materials*. After it is published, it will be found at <https://pubs.aip.org/aip/apm>

In situ Etching of β -Ga₂O₃ using *tert*-Butyl Chloride in an MOCVD System

Cameron A. Gorsak,¹ Henry J. Bowman,² Katie R. Gann,¹ Kathleen T. Smith,³ Jacob Steele,¹ Debdeep Jena,^{1,4,5} Darrell G. Schlom,^{1,5,6} Huili (Grace) Xing,^{1,4,5} Michael O. Thompson,¹ and Hari P. Nair¹

¹Department of Materials Science and Engineering, Cornell University, Ithaca, New York 14853, USA

²PARADIM REU, Cornell University, Ithaca, New York 14853, USA

³School of Applied and Engineering Physics, Cornell University, Ithaca, New York 14853, USA

⁴School of Electrical and Computer Engineering, Cornell University, Ithaca, New York 14853, USA

⁵Kavli Institute at Cornell for Nanoscale Science, Cornell University, Ithaca, New York 14853, USA

⁶Leibniz-Institut für Kristallzüchtung, Max-Born-Str. 2, 12489 Berlin, Germany

In this study, we investigate *in situ* etching of β -Ga₂O₃ in a metal-organic chemical vapor deposition (MOCVD) system using *tert*-Butyl chloride (TBCl). We report the successful etching of both heteroepitaxial ($\bar{2}01$)-oriented and homoepitaxial (010)-oriented β -Ga₂O₃ films over a wide range of substrate temperature, TBCl molar flows, and reactor pressures. We identify that the likely etchant is HCl (g) formed by the pyrolysis of TBCl in the hydrodynamic boundary layer above the substrate. The temperature dependence of the etch rate reveals two distinct regimes characterized by markedly different apparent activation energies. The extracted apparent activation energies suggest that at temperatures below ~ 800 °C the etch rate is likely limited by desorption of etch products, while at higher substrate temperatures chemisorption of HCl limits the etch rate. The relative etch rates of heteroepitaxial ($\bar{2}01$) and homoepitaxial (010) β -Ga₂O₃ were observed to scale by the ratio of the surface energies indicating an anisotropic etch. For (010) homoepitaxial films, relatively smooth post-etch surface morphology was achieved by tuning the etching parameters.

Introduction

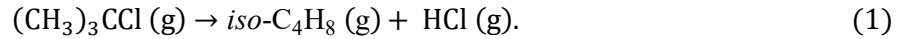
The ultra-wide bandgap semiconductor β -Ga₂O₃ (~ 4.8 eV) has garnered significant attention over the past decade as a platform for devices in power electronics, radio frequency applications, and solar-blind UV photodetectors.¹ The ultra-wide bandgap results in a high critical breakdown field strength yielding a superior Baliga's figure of merit relative to other semiconductors like SiC and GaN.² Progress in β -Ga₂O₃ research has been spurred by the commercial availability of large area (up to 4 inch) melt-grown native substrates³ and the ease of n-type doping.⁴ Metal-organic chemical vapor deposition (MOCVD) has emerged as a technique capable of producing high-quality β -Ga₂O₃ thin films with room-temperature electron mobilities approaching the polar optical phonon limit.⁵⁻⁸ A low-damage *in situ* etch to minimize contamination or plasma-induced damage before subsequent deposition of n+ material⁹ or dielectrics¹⁰ will be key for enabling higher-performance devices. In this study, we investigate the potential of using *tert*-Butyl chloride (TBCl) as a precursor for *in situ* etching of β -Ga₂O₃.

In situ etching of β -Ga₂O₃ has been demonstrated using a flux of elemental gallium in molecular beam epitaxy (MBE) and using triethylgallium (TEGa) in MOCVD.^{11,12} The etch mechanism for both leverages the formation of volatile gallium suboxides via the reaction of elemental gallium with Ga₂O₃.¹³ The use of elemental Ga can, however, potentially leave gallium metal droplets on the surface necessitating an *ex situ* HCl wet etch. *In situ* etching of β -Ga₂O₃ has also been demonstrated in halide vapor phase epitaxy (HVPE) systems using HCl gas.^{14,15}

TBCl is an attractive choice as an etchant precursor since it is relatively noncorrosive compared to HCl, displays long-term stability at room temperature, has a reasonable vapor pressure, and can be installed in the typical bubblers widely used for precursor delivery in MOCVD systems. The first demonstration of *in situ* etching using TBCl was in a chemical beam epitaxy (CBE) system for etching GaAs.^{16,17} Shortly thereafter, *in situ* selective-area etching of InP and its alloys with TBCl in an MOCVD system was used for

the fabrication of buried heterostructure lasers.¹⁸ *In situ* etching using TBCl in MOCVD systems has also been reported for III-V semiconductors such as InGaAs and InAlAs alloys lattice-matched to InP¹⁹ and GaN,²⁰ with smooth surface morphology maintained when the desorption rate of the etch products is greater than the etch rate.

The thermal decomposition of TBCl in the gas phase was studied in the 1930s. Brearley et al.²¹ concluded that below 400 °C and for pressures around 100 Torr, TBCl decomposes via the following pathway:



In this reaction, TBCl pyrolyzes via beta-hydrogen elimination to form *iso*-butene and HCl. Barton and Onyon (1949) later confirmed the production of HCl by titrating their product.²² In 1964, Tsang studied TBCl decomposition via shock tube measurements and employed gas chromatography to identify the gaseous product of the TBCl decomposition reaction, confirming that isobutene and HCl are formed as products during gas-phase pyrolysis of TBCl.²³

Experimental

In situ etching of $\beta\text{-Ga}_2\text{O}_3$ was performed in a cold-wall Agnition Agilis 100 MOCVD system equipped with a remote-injection showerhead. The SiC-coated graphite susceptor was inductively heated and the substrate temperature was measured by a pyrometer aimed at the backside of the susceptor. The etching studies were carried out over reactor pressures of 10 – 60 Torr, susceptor temperatures of 700 – 1000 °C, and TBCl input molar flows of ~20 – 61 $\mu\text{mol}/\text{min}$. The TBCl (99.9999%) was purchased from Dockweiler Chemicals, and the stainless-steel bubbler containing the TBCl was held at a pressure of 900 Torr and a temperature of 5 °C. Both heteroepitaxial ($\bar{2}01$) $\beta\text{-Ga}_2\text{O}_3$, grown on c-plane sapphire, and homoepitaxial films grown on Fe-doped (010) $\beta\text{-Ga}_2\text{O}_3$ from Novel Crystal Technologies were successfully etched. For homoepitaxial films, etching was studied at 15 and 30 Torr, 750 and 875 °C, and a TBCl molar flow of ~61 $\mu\text{mol}/\text{min}$. During etching, Ar (99.999%) was used as a carrier gas and the total flow in the reactor was fixed at 6000 sccm.

UV-vis optical reflectometry was used to measure heteroepitaxial film thickness, while high-resolution X-ray diffraction (XRD) (PANalytical Empyrean) was used to determine homoepitaxial film thickness. Homoepitaxial films grown for determining the etch rate included a thin (~10 nm) $\beta\text{-(Al}_{0.07}\text{Ga}_{0.93})_2\text{O}_3$ interface followed by 200-300 nm of $\beta\text{-Ga}_2\text{O}_3$ which provided an index contrast allowing film thicknesses and etch rates to be determined by Laue oscillations.²⁴ Atomic force microscopy (AFM) was used to evaluate the surface morphology, which was also monitored using Nomarski optical microscopy.

Results and Discussion

We used heteroepitaxial $\beta\text{-Ga}_2\text{O}_3$ grown on c-plane sapphire substrates to map out the etch rate as a function of input TBCl molar flow at several temperatures between 700 and 900 °C (Fig. 1). At a fixed reactor pressure of 15 Torr, we found that etch rate increases nearly linearly with TBCl molar flow between ~20 – 61 $\mu\text{mol}/\text{min}$, which enables fine control of the etch rate.

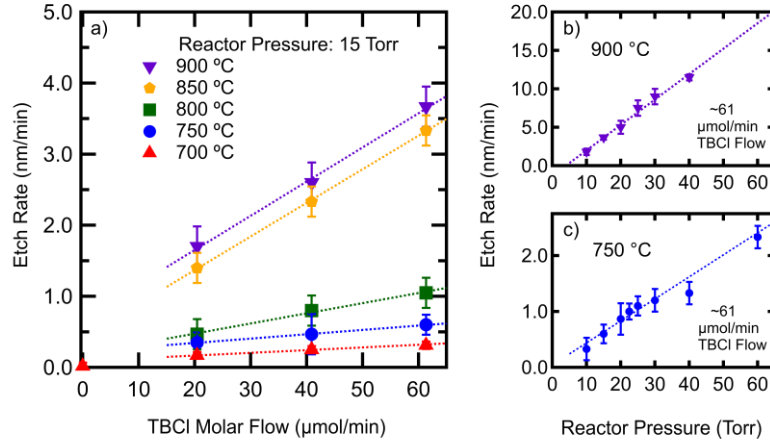


Figure 1. Etch rate of heteroepitaxial β -Ga₂O₃ as a function of a) TBCl molar flow and b-c) reactor pressure. a) At a fixed reactor pressure of 15 Torr and for susceptor temperatures between 700 and 900 °C, increasing the TBCl molar flow results in a linear increase in etch rate. At a fixed TBCl molar flow of ~61 μmol/min, the etch rate monotonically increases with reactor pressure in both the b) high-temperature and c) low-temperature regimes indicating that TBCl etching of β -Ga₂O₃ does not occur in a mass-transport-limited regime.

In general, the etch rate increases with increasing susceptor temperature, however, the slope of the etch rate vs TBCl molar flow jumps sharply from 800 °C to 850 °C, indicative of a sudden change in the etch-limiting step. At a fixed TBCl molar flow of ~61 μmol/min, the etch rate follows an Arrhenius relationship as shown in Fig. 2. There are two distinct activation energy regimes which are commonly observed in CVD growth²⁵ and etching²⁶ processes. In our work, the low-temperature (LT) regime below ~800 °C has a steep apparent activation energy of ~1.48 and ~1.84 eV for 15 and 30 Torr, respectively. The high temperature (HT) regime above ~800 °C exhibits a much lower apparent activation energy of ~0.3 eV. These values are much lower than that required for Ga-O bond dissociation (~3.88 eV)²⁷ and we confirmed that even at the highest etch temperature employed, there is negligible thermal decomposition of gallium oxide²⁸ at the Ar flows and reactor pressures explored in this study.

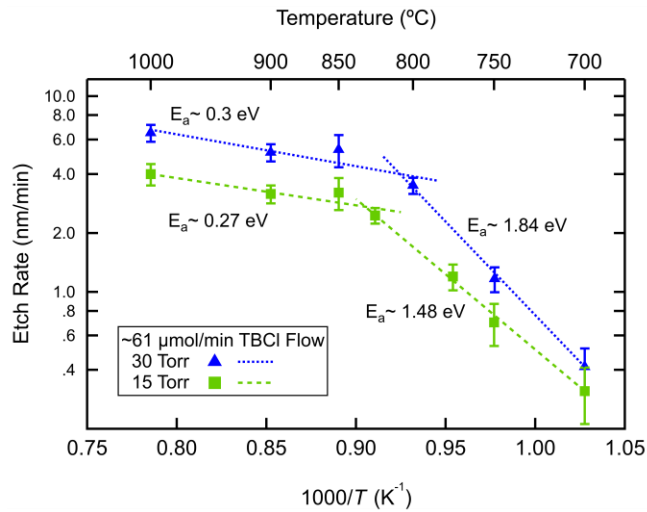


Figure 2. Arrhenius plot of *in situ* etch rate of heteroepitaxial β -Ga₂O₃ on a log scale as a function of inverse temperature for a TBCl molar flow of ~61 μmol/min at reactor pressures of 15 and 30 Torr. The HT and LT etch regimes are delineated by distinct apparent activation energies, likely due to different etch-limiting mechanisms.

During the etching process, the etchant adsorbs on the surface and then reacts to form an etch product, followed by the desorption of the etch product from the surface. Based on the data from Tsang,²³ at temperatures between 700 -1000 °C used in our work and estimated residence times²⁹ for precursors in the heated boundary layer above the susceptor, TBCl is pyrolyzed into isobutene and hydrogen chloride (HCl) (Fig. 3). This temperature range, however, is not high enough to enable further gas-phase pyrolysis of HCl (Fig 3).³⁰ Therefore, it is reasonable to assume that the etchant is HCl and not Cl₂.

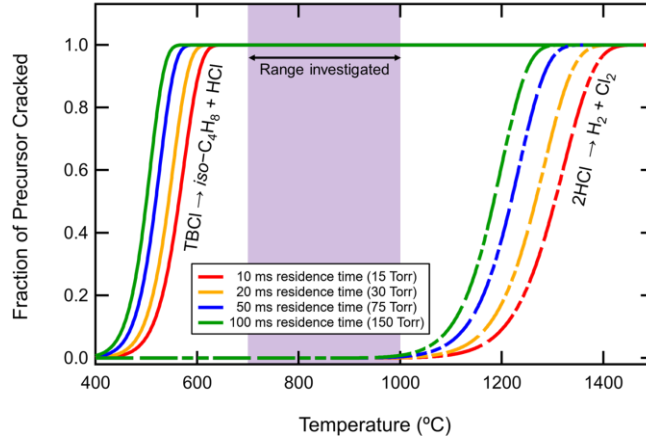
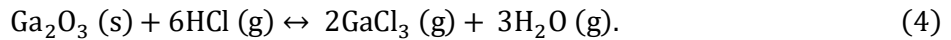
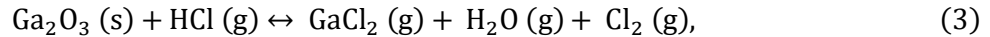
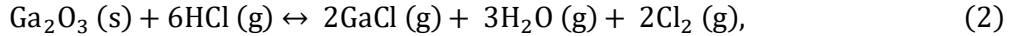


Figure 3. Calculated fraction of TBCl and HCl pyrolyzed as a function of temperature based on typical residence times for precursors in the hot boundary layer above the substrate. The pyrolysis of TBCl into isobutene and hydrogen chloride (HCl) is fully complete by 600 °C, while the thermal decomposition of HCl does not occur until over 1000 °C, illustrating that HCl, generated from the pyrolysis of TBCl, is likely the etchant.

We hypothesize that the HCl formed from the pyrolysis of TBCl adsorbs on the surface of the β -Ga₂O₃ and reacts with Ga₂O₃ to form the GaCl_{*n*} ($n \leq 3$) etch product by one of the following three reactions:



In the LT regime, the weak dependence of etch rate on TBCl molar flow (Fig. 1) suggests the etch is limited by etch product desorption— either GaCl_{*n*} or H₂O. While all thermodynamically favorable gas phase reactions can occur simultaneously, GaCl₃ formation kinetics will depend on the surface coverage of HCl, which is likely to be low given the linear (first order) increase in etch rate with TBCl partial pressure, and the high vapor pressure of HCl even at 700 °C.^{31,32} Therefore, the LT etch product is likely GaCl. Surface science studies of GaCl_{*n*} desorption from GaAs have shown an apparent activation energy for the desorption of GaCl₃ and GaCl of ~0.78 eV and ~1.65 eV,³³ respectively.³⁴ When the apparent activation energy is greater than that expected for the relevant GaCl_{*n*} species, the limiting factor has been attributed to the anionic species (N for GaN and As for GaAs).^{35,36} For the case of β -Ga₂O₃, after the desorption of the volatile GaCl_{*n*} species, the surface is likely left hydroxylated. The hydroxyl-terminated β -Ga₂O₃ surface is observed to be stable to 750 °C in a UHV environment.³⁷ Although the activation energy for the desorption of H₂O from hydroxylated β -Ga₂O₃ is not known at this time, the apparent activation energy for the desorption of H₂O from α -Al₂O₃ surfaces is in the range of ~1.37 - 1.78 eV, which is similar to the value observed in the LT regime.^{38,39} Further studies will be required to more fully elucidate the etch mechanism in the LT regime.

In the HT regime, the dominant GaCl_{*n*} species is most likely GaCl based on thermodynamic calculations of gas phase HVPE growth of GaN with HCl and Ga.⁴⁰ The lower apparent activation energy in the HT regime

is likely not associated with the desorption of etch products, but rather with the activation energy (~ 0.3 eV) for the dissociative adsorption of HCl on the gallium oxide surface.⁴¹ This value is in agreement with the apparent activation energy (~ 0.20 eV and ~ 0.25 eV)^{14,15} extracted above 750 °C from atmospheric pressure HCl etching of β -Ga₂O₃ in an HVPE reactor.

At high substrate temperatures, MOCVD growth typically occurs in a mass-transport-limited regime. In the absence of significant gas-phase parasitic reactions, and when all the flows are held constant, the growth rate is independent of total reactor pressure within this mass-transport-limited regime.⁴² To determine whether etching with TBCl occurs in a mass-transport-regime, the pressure dependence of the etch rate was explored at a fixed TBCl flow rate at two temperatures: 750 °C (LT regime) and 900 °C (HT regime). The reactor pressure was controlled, independent of the total gas flow, using a computer-controlled butterfly valve in the exhaust manifold. Figures 1(b) and 1(c) show that the etch rate is increasing, and not saturating, with increasing reactor pressure indicating that etching is not occurring in a mass-transport-limited regime even at the highest substrate temperatures investigated in this study.

After establishing the trends of *in situ* TBCl etching of β -Ga₂O₃, we explored the relationship between the etch rate of heteroepitaxial ($\bar{2}01$) β -Ga₂O₃ and homoepitaxial (010) β -Ga₂O₃ by etching co-loaded samples under identical conditions. The etch rate for homoepitaxial samples with ~ 61 $\mu\text{mol}/\text{min}$ TBCl molar flow was determined by XRD and is shown in Fig. S2 for four distinct etching conditions (15 Torr at 750 and 875 °C, and 30 Torr at 750 and 875 °C). Figure 4 summarizes these etch rates revealing the anisotropy between the (010) and ($\bar{2}01$) etch rate. Also plotted in Fig. 4 are the ratios between the calculated (010) and ($\bar{2}01$) dangling bonding densities and surface energies which agrees well with the experimental data.⁴³ Similar anisotropy has been observed during *in situ* etching of β -Ga₂O₃ using HCl in an HVPE reactor.¹⁴

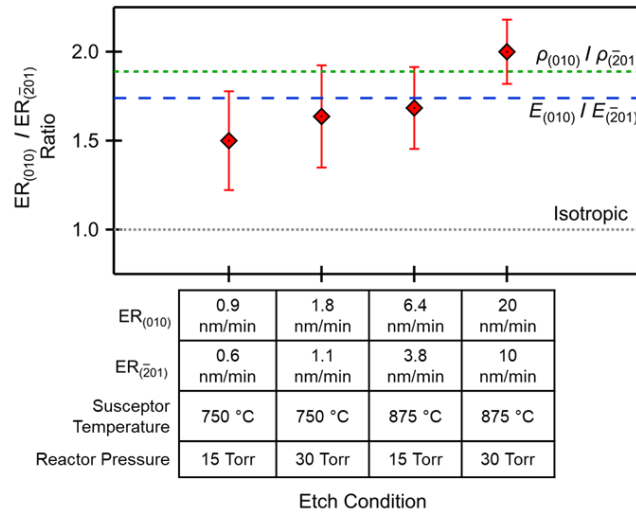


Figure 4. Comparison of etch rate between homoepitaxial (010) β -Ga₂O₃ and heteroepitaxial ($\bar{2}01$) with ~ 61 $\mu\text{mol}/\text{min}$ TBCl molar flow. Included in the plot are the ratios of calculated β -Ga₂O₃ dangling bond densities (ρ , green) and surface energies (E , blue) from Mu *et al.* (2020) illustrating that the anisotropy of the etch rate is correlated with the surface energy anisotropy: the higher the surface energy, the higher the etch rate.

To investigate the surface morphology of *in situ* etched gallium oxide thin films, ~ 400 nm thick homoepitaxial (010) unintentionally doped (UID) β -Ga₂O₃ samples were grown and then immediately *in situ* etched, without cooling down, to a depth of ~ 100 nm for each of the four conditions shown in Fig. 5(b-e). The resulting surface morphology resembles that resulting from hot phosphoric wet etching⁴⁴ and does not exhibit characteristic faceting of the (110) plane along the [001] direction typically seen post-growth⁴⁵

(as shown for an unetched film in Fig. S2(b)) or after elemental Ga etching.^{11,12} In general we observe that etching under higher reactor pressures and low substrate temperatures results in smoother surface morphologies. The smoothest surface, with an RMS roughness of 2.56 nm, was observed for etching at 750 °C, 15 Torr. At this time, the exact mechanism for surface roughening is unclear but we note that the reactor parameters for smoother etch morphologies also result in longer surface residence time of etchant and etch products. We have also demonstrated that subsequent regrowth after an *in situ* etch results in sub-nanometer RMS roughness, as shown in Fig. S3.

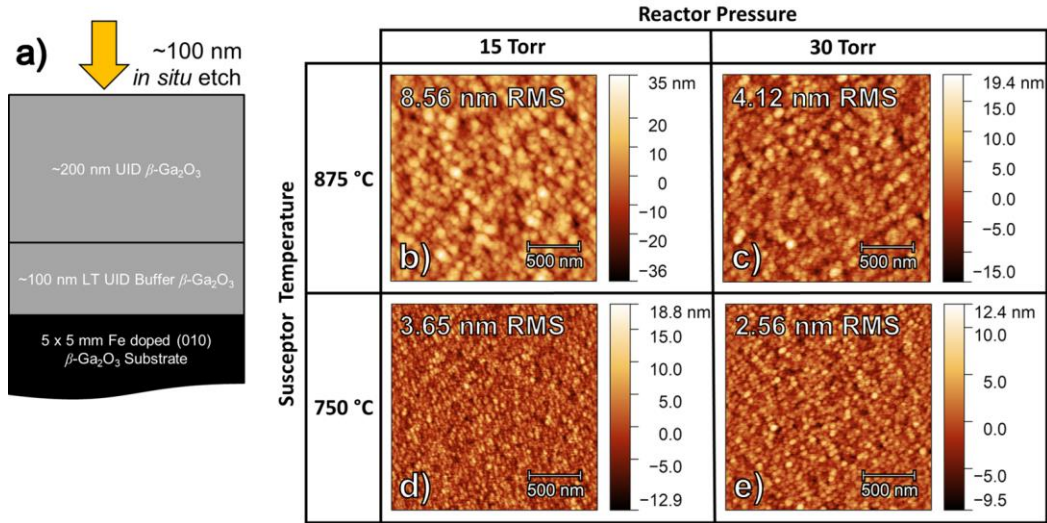


Figure 5. Surface morphologies of *in situ* TBCl etched β -Ga₂O₃. a) Layer structure illustrating ~100 nm *in situ* etch after growth of ~400 nm of UID β -Ga₂O₃ on Fe-doped (010) substrates. b-e) AFM of surfaces after etching with ~61 μ mol/min TBCl molar flow at various conditions. The 750 °C etch (bottom row) is smoother than etching at 875 °C (top row). 30 Torr etching (right column) is smoother than 15 Torr (left column).

Conclusion

In summary, this study investigated the *in situ* etching of both heteroepitaxial ($\bar{2}01$) and homoepitaxial (010) β -Ga₂O₃ films by TBCl in an MOCVD system over a susceptor temperature range of 700 – 1000 °C, reactor pressure of 10 – 60 Torr, and TBCl molar flow of ~20 – 61 μ mol/min. Two distinct regimes for TBCl etching of β -Ga₂O₃ were observed. The LT regime, below ~800 °C, exhibits an apparent activation energy of ~1.48 and ~1.84 eV for 15 and 30 Torr, respectively. In the LT regime, we hypothesize the etch rate is limited by the desorption of GaCl_n, or likely H₂O. In the HT regime, we hypothesize the thermodynamically favored etch product is GaCl and the lower apparent activation energy ~0.3 eV is likely associated with the dissociative adsorption of HCl on the surface. The relationship between the etch rate of ($\bar{2}01$) and (010) β -Ga₂O₃ scales by the ratio of surface energies. Finally, the surface morphology of *in situ* etched homoepitaxial (010) β -Ga₂O₃ films was evaluated and it was determined that the lower temperature, higher pressure etch resulted in smoother surfaces. This work, in which successful *in situ* etching of β -Ga₂O₃ with TBCl is demonstrated, lays the groundwork for utilizing *in situ* etching and regrowth to obtain low contact resistance ohmic contacts and improve β -Ga₂O₃ device performance.

Acknowledgments

We acknowledge support from the AFOSR/AFRL ACCESS Center of Excellence under Award No. FA9550-18-10529. C.A.G acknowledges support from the National Defense Science and Engineering Graduate (NDSEG) Fellowship. H.J.B. acknowledges support from the National Science Foundation (NSF) [Platform for the Accelerated Realization, Analysis and Discovery of Interface Materials (PARADIM)] under Cooperative Agreement No. DMR-1539918. We also acknowledge support from PARADIM for XRD usage. Substrate dicing and AFM were performed in the Cornell NanoScale Facility, a member of the National Nanotechnology Coordinated Infrastructure (NNCI), which is supported by the NSF (Grant No. NNCI-2025233).

Author Contributions

C. A. Gorsak and H. J. Bowman contributed equally to this paper.

References:

- ¹ M. J. Tadjer, "Toward gallium oxide power electronics." *Science* 378, 724–725 (2022). <https://doi.org/10.1126/science.add2713>
- ² M. Higashiwaki, K. Sasaki, A. Kuramata, T. Masui, and S. Yamakoshi. "Development of gallium oxide power devices," *physica status solidi (a)* 211, 21–26 (2014). <https://doi.org/10.1002/pssa.201330197>
- ³ A. Kuramata, K. Koshi, S. Watanabe, Y. Yamaoka, T. Masui, & S. Yamakoshi, "Bulk crystal growth of Ga₂O₃," *Proc. SPIE* 10533, 105330E (2018). <https://doi.org/10.1117/12.2301405>
- ⁴ Y. Zhang, and J.S. Speck, "Importance of shallow hydrogenic dopants and material purity of ultra-wide bandgap semiconductors for vertical power electron devices," *Semiconductor Science and Technology*, 35(12), 125018 (2020). <https://doi.org/10.1088/1361-6641/abba6>
- ⁵ A. Bhattacharyya, C. Peterson, T. Itoh, S. Roy, J. Cooke, S. Rebollo, P. Ranga, B. Sensale-Rodriguez, and S. Krishnamoorthy, "Enhancing the electron mobility in Si-doped (010) β -Ga₂O₃ films with low-temperature buffer layers," *APL Mater* 11 (2), 021110 (2023). <https://doi.org/10.1063/5.0137666>
- ⁶ Y. Zhang, F. Alema, A. Mauze, O. S. Koksaldi, R. Miller, A. Osinsky, and J. S. Speck, "MOCVD grown epitaxial β -Ga₂O₃ thin film with an electron mobility of 176 cm²/V s at room temperature," *APL Mater* 7 (2), 022506 (2019). <https://doi.org/10.1063/1.5058059>
- ⁷ L. Meng, Z. Feng, A. F. M. A. Uddin Bhuiyan, and H. Zhao, "High-Mobility MOCVD β -Ga₂O₃ Epitaxy with Fast Growth Rate Using Trimethylgallium," *Cryst. Growth Des.* 22 (6), 3896–3904 (2022). <https://doi.org/10.1021/acs.cgd.2c00290>
- ⁸ N. Ma, N. Tanen, A. Verma, Z. Guo, T. Luo, H. Xing, and D. Jena, "Intrinsic electron mobility limits in β -Ga₂O₃," *Appl. Phys. Lett.* 109, 212101 (2016). <https://doi.org/10.1063/1.4968550>
- ⁹ Z. Xia, C. Joishi, S. Krishnamoorthy, S. Bajaj, Y. Zhang, M. Brenner, S. Lodha, and S. Rajan, "Delta doped β -Ga₂O₃ field effect transistors with regrown ohmic contacts," *IEEE Electron Device Lett.* 39, 568–571 (2018). <https://doi.org/10.1109/LED.2018.2805785>
- ¹⁰ N. K. Kalarickal, A. Dheenan, J. F. McGlone, S. Dhara, M. Brenner, S. A. Ringel, and S. Rajan, "Demonstration of self-aligned β -Ga₂O₃ δ -doped MOSFETs with current density >550 mA/mm," *Appl. Phys. Lett.* 122, 113506 (2023). <https://doi.org/10.1063/5.0131996>
- ¹¹ N. K. Kalarickal, A. Fiedler, S. Dhara, H.-L. Huang, A. F. M. A. U. Bhuiyan, M. W. Rahman, T. Kim, Z. Xia, Z. J. Eddine, A. Dheenan, M. Brenner, H. Zhao, J. Hwang, and S. Rajan, "Planar and three-dimensional damage-free etching of β -Ga₂O₃ using atomic gallium flux," *Appl. Phys. Lett.* 119 (12), 123503 (2021). <https://doi.org/10.1063/5.0057203>
- ¹² A. Katta, F. Alema, W. Brand, A. Gilankar, A. Osinsky, and N.K. Kalarickal, "Demonstration of MOCVD based *in situ* etching of β -Ga₂O₃ using TEGa," *Journal of Applied Physics* 135(7), 075705 (2024). <https://doi.org/10.1063/5.0195361>
- ¹³ P. Vogt, F.V.E. Hensling, K. Azizie, C.S. Chang, D. Turner, J. Park, J.P. McCandless, H. Paik, B.J. Bocklund, G. Hoffman, O. Bierwagen, D. Jena, H.G. Xing, S. Mou, D.A. Muller, S.-L. Shang, Z.-K. Liu, and D.G. Schlom, "Adsorption-controlled growth of Ga₂O₃ by suboxide molecular-beam epitaxy," *APL Materials* 9(3), 031101 (2021). <https://doi.org/10.1063/5.0035469>
- ¹⁴ T. Oshima, and Y. Oshima, "Plasma-free dry etching of (001) β -Ga₂O₃ substrates by HCl gas," *Applied Physics Letters* 122(16), 162102 (2023). <https://doi.org/10.1063/5.0138736>
- ¹⁵ Y. Oshima, and T. Oshima, "Effect of the temperature and HCl partial pressure on selective-area gas etching of (001) β -Ga₂O₃," *Jpn. J. Appl. Phys.* 62, 080901 (2023). <https://doi.org/10.35848/1347-4065/acee3b>
- ¹⁶ M. Kondow, B. Shi, and C.W. Tu, "Chemical Beam Etching of GaAs Using a Novel Precursor of Tertiarybutylchloride (TBCl)," *Jpn. J. Appl. Phys.* 38, L617 (1999). <https://doi.org/10.1143/JJAP.38.L617>
- ¹⁷ M. Kondow, B. Shi, and C.W. Tu, "In situ etching using a novel precursor of tertiarybutylchloride (TBCl)," *Journal of Crystal Growth* 209(2), 263–266 (2000). [https://doi.org/10.1016/S0022-0248\(99\)00552-7](https://doi.org/10.1016/S0022-0248(99)00552-7)
- ¹⁸ P. Wolfram, W. Ebert, J. Kreissl, and N. Grote, "MOVPE-based in situ etching of In(GaAs)P/InP using tertiarybutylchloride," *Journal of Crystal Growth* 221(1), 177–182 (2000). [https://doi.org/10.1016/S0022-0248\(00\)00682-5](https://doi.org/10.1016/S0022-0248(00)00682-5)
- ¹⁹ S. Codato, R. Campi, C. Rigo, and A. Stano, "Ga-assisted in situ etching of AlGaInAs and InGaAsP multi-quantum well structures using tertiarybutylchloride," *Journal of Crystal Growth* 282, 7-17 (2005). <https://doi.org/10.1016/j.jcrysgro.2005.04.080>
- ²⁰ B. Li, M. Nami, S. Wang, and J. Han, "In situ and selective area etching of GaN by tertiarybutylchloride (TBCl)," *Appl. Phys. Lett.* 115(16), 162101 (2019). <https://doi.org/10.1063/1.5120420>
- ²¹ D. Brearley, G. B. Kistiakowsky, and C. H. Stauffer, "The Thermal Decomposition of Tertiary Butyl and Tertiary Amyl Chlorides, Gaseous Homogeneous Unimolecular Reactions," *J. Am. Chem. Soc.* 58(1), 43–47 (1936). <https://doi.org/10.1021/ja01292a011>
- ²² D. H. R. Barton and P. F. Onyon, "The Kinetics of the Dehydrochlorination of Substituted Hydrocarbons. Part IV. The mechanism of the Thermal Decomposition of Tert.-Butyl Chloride," *Transactions of the Faraday Society* 45, 725-735 (1949). <https://doi.org/10.1039/TF9494500725>
- ²³ W. Tsang, "Thermal Decomposition of Some Tert-Butyl Compounds at Elevated Temperatures," *J. Chem. Phys.* 40, 1498–1505 (1964). <https://doi.org/10.1063/1.1725353>
- ²⁴ T. Itoh, A. Mauze, Y. Zhang, and J. S. Speck, "Epitaxial growth of β -Ga₂O₃ on (110) substrate by plasma-assisted molecular beam epitaxy," *Appl. Phys. Lett.* 117(15), 152105 (2020). <https://doi.org/10.1063/5.0027884>
- ²⁵ M. Liehr, C.M. Greenlief, S.R. Kasi, and M. Offenber, "Kinetics of silicon epitaxy using SiH₄ in a rapid thermal chemical vapor deposition reactor," *Appl. Phys. Lett.* 56(7), 629–631 (1990). <https://doi.org/10.1063/1.102719>
- ²⁶ A. Rebey, A. Bchetnia, and B. El Jani, "Etching of GaAs by CCl₄ and VCl₄ in a metalorganic vapor-phase epitaxy reactor," *Journal of Crystal Growth* 194(3), 286–291 (1998). [https://doi.org/10.1016/S0022-0248\(98\)00606-X](https://doi.org/10.1016/S0022-0248(98)00606-X)
- ²⁷ W.-L. Huang, Y.-Z. Lin, S.-P. Chang, W.-C. Lai, and S.-J. Chang, "Stability-Enhanced Resistive Random-Access Memory via Stacked In_xGa_{1-x}O by the RF Sputtering Method," *ACS Omega* 6(16), 10691–10697 (2021). <https://doi.org/10.1021/acsomega.1c00112>
- ²⁸ S. Lany, "Defect phase diagram for doping of Ga₂O₃," *APL Materials* 6(4), 046103 (2018). <https://doi.org/10.1063/1.5019938>
- ²⁹ L. Hui, "Mass transport analysis of a showerhead MOCVD reactor," *J. Semicond.* 32(3), 033006 (2011). <https://doi.org/10.1088/1674-4926/32/3/033006>
- ³⁰ G.N. Schading, and P. Roth, "Thermal decomposition of HCl measured by ARAS and IR diode laser spectroscopy." *Combustion and Flame* 99(3-4), 467-474.(1994). [https://doi.org/10.1016/0010-2180\(94\)90038-8](https://doi.org/10.1016/0010-2180(94)90038-8)
- ³¹ C. Su, M. Xi, Z-G. Dai, M. F. Vernon, and B.E. Bent, "Dry etching of GaAs with Cl₂: Correlation between the surface Cl coverage and the etching rate at steady state," *Surface science* 282(3), 357-370. (1993). [https://doi.org/10.1016/0039-6028\(93\)90940-L](https://doi.org/10.1016/0039-6028(93)90940-L)

-
- ³² T. Senga, Y. Matsumi, and M. Kawasaki, "Chemical dry etching mechanisms of GaAs surface by HCl and Cl₂," *Journal of Vacuum Science & Technology B: Microelectronics and Nanometer Structures Processing, Measurement, and Phenomena* 14(5), 3230–3238 (1996). <https://doi.org/10.1116/1.588812>
- ³³ C. Sasaoka, Y.K.Y. Kato, and A.U.A. Usui, "Thermal Desorption of Galliumchloride Adsorbed on GaAs (100)," *Jpn. J. Appl. Phys.* 30(10A), L1756 (1991). <https://doi.org/10.1143/JJAP.30.L1756>
- ³⁴ C.L. French, W.S. Balch, and J.S. Foord, "Investigations of the thermal reactions of chlorine on the GaAs (100) surface," *Journal of Physics: Condensed Matter*, 3(S), S351. (1991). <https://doi.org/10.1088/0953-8984/3/S/054>
- ³⁵ D. Fahlé, T. Kruecken, M. Dauelsberg, H. Kalisch, M. Heuken, and A. Vescan, "*In-situ* decomposition and etching of AlN and GaN in the presence of HCl," *Journal of crystal growth*, 393, 89-92. (2014). <https://doi.org/10.1016/j.jcrysgro.2013.09.025>
- ³⁶ J.M. Ortion, Y. Cordier, J.Ch. Garcia, and C. Grattepain, "Temperature dependence of GaAs chemical etching using AsCl₃," *Journal of Crystal Growth* 164(1), 97–103 (1996). [https://doi.org/10.1016/0022-0248\(95\)01019-X](https://doi.org/10.1016/0022-0248(95)01019-X)
- ³⁷ R.M. Gazoni, L. Carroll, J.I. Scott, S. Astley, D.A. Evans, A.J. Downard, R.J. Reeves, and M.W. Allen, "Relationship between the hydroxyl termination and band bending at (201) β -Ga₂O₃ surfaces," *Phys. Rev. B* 102(3), 035304 (2020). <https://doi.org/10.1103/PhysRevB.102.035304>
- ³⁸ Z. Łodziana, J.K. Nørskov, and P. Stoltze, "The stability of the hydroxylated (0001) surface of α -Al₂O₃," *The Journal of Chemical Physics* 118(24), 11179–11188 (2003). <https://doi.org/10.1063/1.1574798>
- ³⁹ C.E. Nelson, J.W. Elam, M.A. Cameron, M.A. Tolbert, and S.M. George, "Desorption of H₂O from a hydroxylated single-crystal α -Al₂O₃(0001) surface," *Surface Science* 416(3), 341–353 (1998). [https://doi.org/10.1016/S0039-6028\(98\)00439-7](https://doi.org/10.1016/S0039-6028(98)00439-7)
- ⁴⁰ W. Seifert, G. Fitzl, and E. Butter, "Study on the growth rate in VPE of GaN," *Journal of Crystal Growth* 52, 257–262 (1981). [https://doi.org/10.1016/0022-0248\(81\)90201-3](https://doi.org/10.1016/0022-0248(81)90201-3)
- ⁴¹ K.N. Nigussa, K.L. Nielsen, Ø. Borck, and J.A. Støvneng, "Adsorption of H₂, Cl₂, and HCl molecules on α -Cr₂O₃(0001) surfaces: A density functional theory investigation," *Surface Science* 653, 211–221 (2016). <https://doi.org/10.1016/j.susc.2016.07.004>
- ⁴² C.H. Chen, H. Liu, D. Steigerwald, W. Imler, C.P. Kuo, M.G. Craford, M. Ludowise, S. Lester, and J. Amano, "A study of parasitic reactions between NH₃ and TMGa or TMAI," *J. Electron. Mater.* 25(6), 1004–1008 (1996). <https://doi.org/10.1007/BF02666736>
- ⁴³ S. Mu, M. Wang, H. Peelaers, and C.G. Van de Walle, "First-principles surface energies for monoclinic Ga₂O₃ and Al₂O₃ and consequences for cracking of (Al_xGa_{1-x})₂O₃," *APL Materials* 8(9), 091105 (2020). <https://doi.org/10.1063/5.0019915>
- ⁴⁴ Y. Zhang, A. Mauze, and J.S. Speck, "Anisotropic etching of β -Ga₂O₃ using hot phosphoric acid," *Appl. Phys. Lett.* 115(1), 013501 (2019). <https://doi.org/10.1063/1.5093188>
- ⁴⁵ P. Mazzolini, and O. Bierwagen, "Towards smooth (010) β -Ga₂O₃ films homoepitaxially grown by plasma assisted molecular beam epitaxy: The impact of substrate offset and metal-to-oxygen flux ratio," *Journal of Physics D: Applied Physics* 53(35), 354003. (2020). <https://doi.org/10.1088/1361-6463/ab8eda>

Supplementary Material

In situ Etching of β -Ga₂O₃ using *tert*-Butyl Chloride in an MOCVD System

Cameron A. Gorsak,¹ Henry J. Bowman,² Katie R. Gann,¹ Kathleen T. Smith,³ Jacob Steele,¹ Debdeep Jena,^{1,4,5} Darrell G. Schlom,^{1,5,6} Huili (Grace) Xing,^{1,4,5} Michael O. Thompson,¹ and Hari P. Nair¹

¹Department of Materials Science and Engineering, Cornell University, Ithaca, New York 14853, USA

²PARADIM REU, Cornell University, Ithaca, New York 14853, USA

³School of Applied and Engineering Physics, Cornell University, Ithaca, New York 14853, USA

⁴School of Electrical and Computer Engineering, Cornell University, Ithaca, New York 14853, USA

⁵Kavli Institute at Cornell for Nanoscale Science, Cornell University, Ithaca, New York 14853, USA

⁶Leibniz-Institut für Kristallzüchtung, Max-Born-Str. 2, 12489 Berlin, Germany

Effect of O₂ on Etch Rate

In order to investigate the effect of oxygen on etch rate we introduced a 50 sccm flow of O₂ into the reactor during etching. In the LT regime, the etch rate was largely not affected, however, in the HT regime the etch rate was suppressed by a factor of ~ 2 as seen in Fig. S1. We believe that the HT etch rate is suppressed due to the competing HVPE growth back reaction. Additional O₂ is also expected to lead to rougher surfaces as experienced in the TBCl etching of GaN with additional NH₃ flow.¹

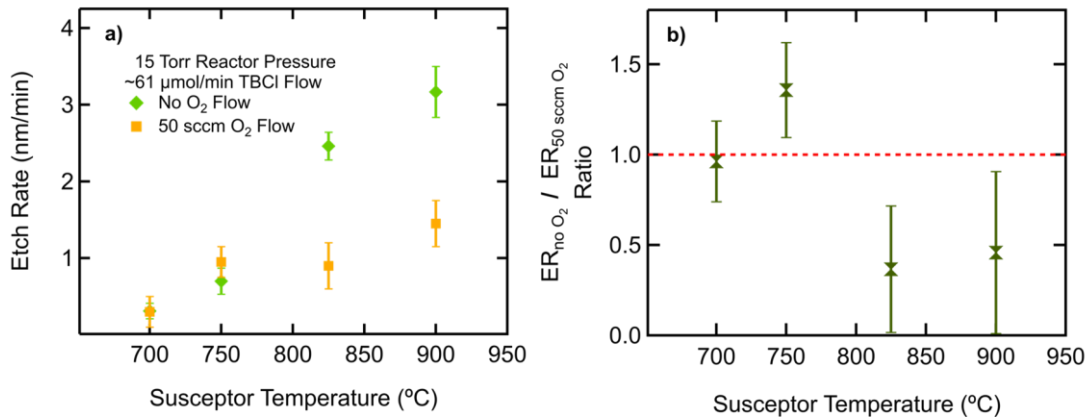


Figure S1. Effect of additional O₂ flow on etch rate. a) Etch rate as a function of susceptor temperature with no O₂ (green) and with 50 sccm O₂ flow (yellow). b) Ratio of the etch rate without oxygen divided by the etch rate with oxygen vs susceptor temperature. Below 800 °C the etch rate is relatively unchanged but is suppressed at higher temperatures.

Homoepitaxial Growth Conditions and Etch Rate Determination

All layers were grown at a reactor pressure of 15 Torr. Triethylgallium (TEGa), triethylaluminum (TEAl), and O_2 were used as precursors. The LT UID buffers were grown at 600 °C with a typical TEGa and O_2 flow of $\sim 38.5 \mu\text{mol}/\text{min}$ and 500 sccm, respectively. The 800 °C UID layers were grown with a typical TEGa and O_2 flow of $\sim 77 \mu\text{mol}/\text{min}$ and 400 sccm, respectively. The growth of the heteroepitaxial samples was similar.

A thin ($\sim 10 \text{ nm}$) layer of $\beta\text{-(Al}_{0.07}\text{Ga}_{0.93})_2\text{O}_3$ serves as an interface to separate the $\beta\text{-Ga}_2\text{O}_3$ film from the underlying substrate so that thickness fringes from the $\sim 200\text{-}300 \text{ nm}$ thick film of $\beta\text{-Ga}_2\text{O}_3$ can be seen in $\theta\text{-}2\theta$ XRD scans (Fig. S2(c-f)). Laue oscillations were used to determine the thickness. The thin $\beta\text{-(Al}_{0.07}\text{Ga}_{0.93})_2\text{O}_3$ layers were grown at 705 °C with a TEGa and O_2 flow of $\sim 80 \mu\text{mol}/\text{min}$ and 200 sccm, respectively. The TEGa:TEAl input ratio was ~ 16 .

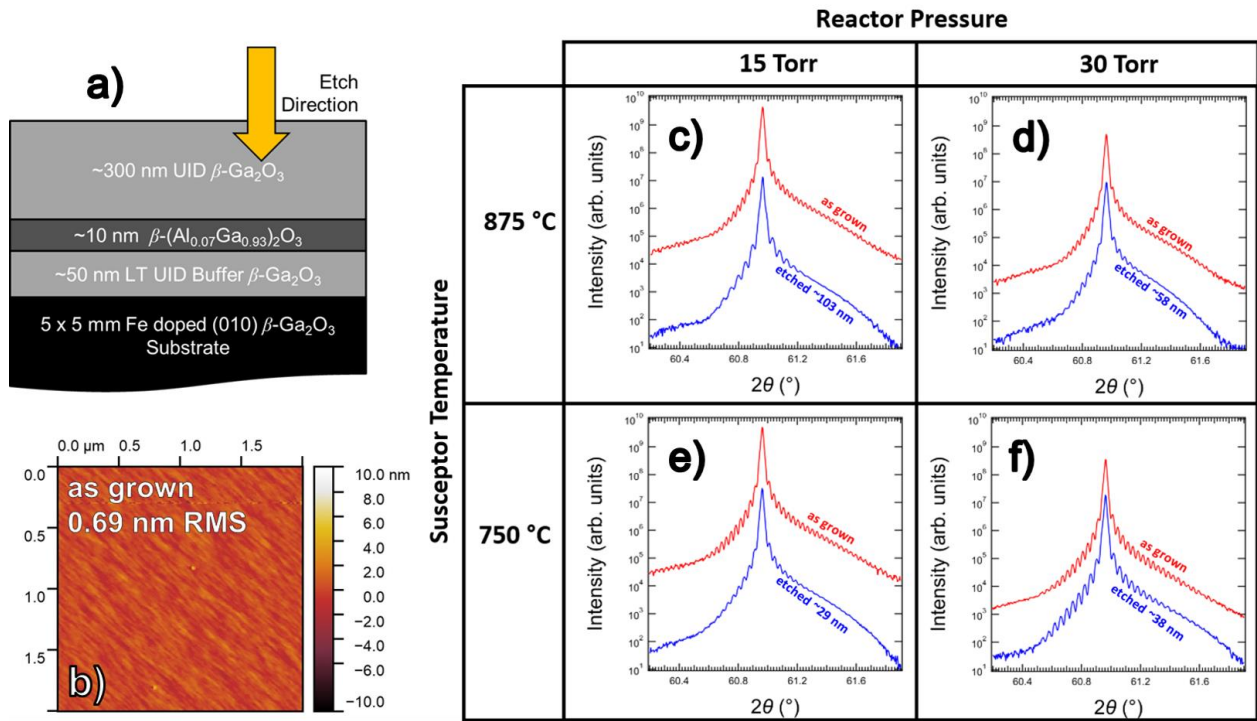


Figure S2. Etch rate determination of homoepitaxial (010) $\beta\text{-Ga}_2\text{O}_3$. a) Layer structure of as-grown sample. b) AFM of an as-grown and not etched (010) $\beta\text{-Ga}_2\text{O}_3$ film surface indicating sub-nanometer RMS roughness c-f) XRD of pre- and post-etched samples. Etching was done with $\sim 61 \mu\text{mol}/\text{min}$ input TBCl molar flow at various conditions: 750 °C (bottom row), 875 °C (top row), 30 Torr (right column), and 15 Torr (left column). Laue oscillations were used to determine the thicknesses.

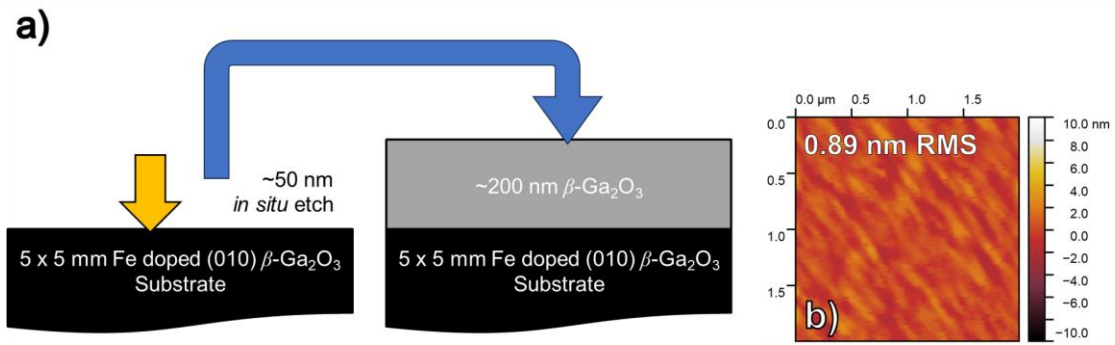


Figure S3. a) Layer structure of immediate regrowth after ~ 50 nm *in situ* TBCl etch with ~ 61 $\mu\text{mol}/\text{min}$ input molar flow at 875 $^{\circ}\text{C}$ and 30 Torr. b) AFM of the surface after regrowth showcasing sub-nanometer RMS roughness.

Reference:

¹ B. Li, M. Nami, S. Wang, and J. Han, "*In situ* and selective area etching of GaN by tertiarybutylchloride (TBCl)," *Appl. Phys. Lett.* 115(16), 162101 (2019). <https://doi.org/10.1063/1.5120420>